

## Tempering behavior of iron-nitrogen-based martensite

Mitsutaka Sato<sup>1\*</sup>, Tadashi Furuhashi<sup>1</sup>

<sup>1</sup> Institute for Materials Research, Tohoku University, 2-1-1 Katahira, Aoba-ku, Sendai 980-8577, Japan

**Abstract:** The tempering behaviors of nitrogen (N) martensite have been carried out mainly in stainless steels and high nitrogen binary alloys so far, and the influence of alloying element in low alloys has not been clarified yet. In this study, the tempering behavior of iron-nitrogen-based martensitic alloys containing 0.3 mass%N at temperatures between 100 °C and 550 °C was investigated by quantitative analysis of the corresponding changes in hardness and volume fraction of precipitates. The Vickers hardness was around 500 HV for of as-quenched specimens, and monotonously decreased to 300 HV with increasing tempering temperature due to the precipitation of  $\alpha''$ -Fe<sub>16</sub>N<sub>2</sub> at the low tempering temperature region and that of  $\gamma'$ -Fe<sub>4</sub>N at high tempering temperature region in the case of the Fe-0.3N alloy. The Si-added alloy shows similar tendency to the Fe-0.3N alloy whereas the Mo or Mn-added alloys show resistance to temper softening at temperatures above 300 °C. On the other hand, in the Cr-added alloy, hardness significantly increases upon tempering at temperatures above 300 °C.

### 1. INTRODUCTION

Structural steels require having a good balance of strength and toughness. Martensitic steels are industrially very important because of their very high strength. However they also tend to be brittle in as-quenched conditions, and an optimum balance of strength and toughness is provided by tempering heat treatment. The effect of nitrogen on the martensitic transformation has been investigated in various nitrogen-bearing martensitic steels so far. Fe-C and Fe-N martensites have been found to have much in common in terms of lattice parameter, Ms temperature, and dislocation density under the same carbon/nitrogen content [1-2]. It also has been reported that as-quenched Fe-N martensite decomposes by tempering in the following processes [3]. (1) transformation of retained austenite into martensite in the temperature range between -160 °C and -40 °C, (2) segregation and ordering of nitrogen atoms below 100 °C, (3) precipitation of incoherent  $\alpha''$ -Fe<sub>16</sub>N<sub>2</sub> between 100 °C and 220 °C, (4) conversion of  $\alpha''$ -Fe<sub>16</sub>N<sub>2</sub> into  $\gamma'$ -Fe<sub>4</sub>N between 220 °C and 290 °C, and (5) decomposition of retained austenite between 240 °C and 350 °C. This tempering behavior is quite similar to Fe-C alloy. For the influence of alloying elements in nitrogen martensite, there have been many kinds of researches using high Cr steel with a focused on stainless steel [4]. Tsuchiyama et al. investigated the influence of nitrogen and carbon addition in martensitic stainless steels and reported that both alloys have lath martensite structure and there is a difference in packet size in the interstitial element concentration range of 0 to 0.3 mass% [5]. In addition, Berns et al. investigated the influence of nitrogen and carbon on the tempering behavior of 15mass%Cr-1mass%Mo steel, and significant secondary hardening in nitrogen steel due to the precipitation of CrN by tempering at 450 °C was reported [6].

As described above, most of the studies on tempering behavior of nitrogen martensite have been performed for high nitrogen Fe-N binary alloys and stainless steels. Therefore, the influence of alloying element in low alloy steels has not been clarified yet. In this study, the tempering behavior of iron-nitrogen-based martensitic alloys containing 0.3 mass%N at temperatures between 100 °C and 550 °C was investigated by quantitative analysis of the corresponding changes in hardness and volume fraction of precipitates.

### 2. EXPERIMENTAL PROCEDURE

Pure iron and Fe-1mass%M (M : Si, Cr, Mn, Mo) alloys were used as starting materials. The composition of these alloy is listed in Table 1. Each alloy was homogenized and cut and polished into the dimensions of 14<sup>h</sup> × 8<sup>w</sup> × 0.5<sup>t</sup> mm. After rinsing with acetone, they were subjected to N-Q treatment [7] to obtain nitrogen-containing martensite. During the N-Q treatment, a mixed gas of H<sub>2</sub> and NH<sub>3</sub> was

---

\* Corresponding author. E-mail: m-sato@imr.tohoku.ac.jp, telephone: +81 22 215 2231.

Table 1 Composition of starting materials

	C	Si	Mn	P	S	Cr	Mo	S. Al
Pure Fe	0.011	0.02	0.02	0.001	0.003	0.01	< 0.01	< 0.001
Fe-1Mn	0.001	0.01	0.98	< 0.001	< 0.001	-	-	-
Fe-1Cr	0.01	0.02	0.02	0.001	0.003	0.99	0.01	< 0.001
Fe-1Si	0.001	0.95	0.01	< 0.001	< 0.001	-	-	-
Fe-1Mo	0.01	0.02	0.02	0.002	0.003	0.01	0.97	< 0.001

used and the total gas flux was fixed to 100 ml/min at atmospheric pressure. Treatment temperature, treatment time and introduced ammonia partial pressure were varied for each alloy. After nitriding treatment, the specimen was quenched into iced water. Detailed N-Q treatment conditions are shown in Table 2. Weight change before and after N-Q treatment was measured using precision electronic balance and the amount of nitrogen introduced into the sample by the nitriding treatment was estimated and only the sample with a nitrogen content of 0.3 mass% ( $\pm 5\%$ ) was used to tempering. Tempering treatment was conducted using both of an oil bath and a salt bath in the temperature range between 100 °C and 550 °C for 60 min. The microstructures of those specimens were observed by optical microscope and scanning electron microscope (SEM). Phase identification and measurements of lattice parameters, dislocation densities, and volume fractions were made by X-ray diffraction (XRD) using Co target ( $\lambda : 1.7889 \text{ \AA}$ ). The volume fraction of was estimated using follows equation;

$$V_{\gamma'} = \frac{I_{\gamma'}/R_{\gamma'}}{I_{\gamma'}/R_{\gamma'} + I_{\alpha}/R_{\alpha}}$$

where,  $V_{\gamma'}$  is volume fraction of  $\gamma'$ -Fe<sub>4</sub>N,  $R_{\gamma'}$  and  $R_{\alpha}$  are the ideal peak intensity of  $\gamma'$ -Fe<sub>4</sub>N and ferrite phase, and  $I_{\gamma'}$  and  $I_{\alpha}$  are the measured intensity of  $\gamma'$ -Fe<sub>4</sub>N and ferrite phase, respectively. The hardness of specimen was measured by a micro Vickers tester.

Table 2 Preparation condition of specimen by N-Q treatment

Alloy	$P_{\text{NH}_3}$ (atm)	Temperature (°C)	Time (min)
Pure Fe	0.20	1000	60
Fe-1Si	0.14		
Fe-1Cr	0.10		
Fe-1Mo	0.18	945	120
Fe-1Mn	0.20		

### 3. RESULTS AND DISCUSSION

Fig. 1 shows SEM images of as-quenched and tempered Fe-0.3N specimens. A typical lath martensite structure was observed, and precipitates were not found in the prior austenite grain and its boundaries. Needle- or plate-like precipitates were observed at the lath boundary, inside the lath and the prior austenite grain boundary after tempering, and they were coarsened at 500 °C (Fig. 1 (d)). In addition, precipitates formed by tempering at 100 °C were generated so as to be orthogonal to each other in the block and it is thought that these precipitates have a specific orientation relationship with the matrix. The Si, Mn and Mo-added specimens also showed similar precipitation behavior to the Fe-0.3N specimen. On the other hand, in the case of the Cr-added alloy, these precipitates were observed in the tempered specimen at low temperature, however the amount of precipitates remarkably decreased by increasing tempering temperature.

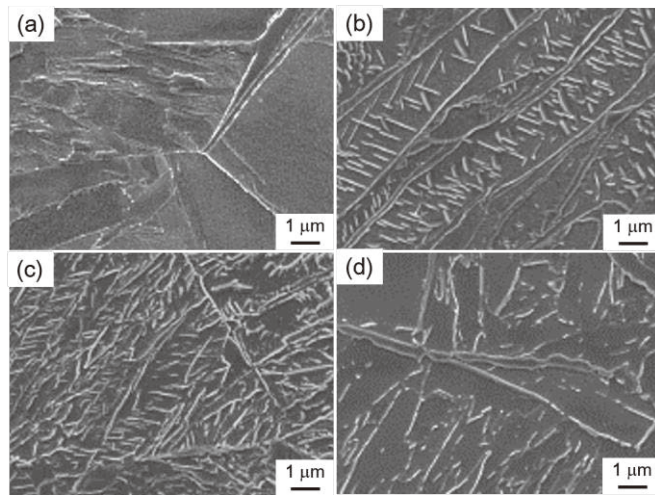


Fig. 1 SEM images of Fe-0.3N specimen. (a) as-quenched, tempered at (b) 100 °C, (c) 300 °C and (d) 500 °C.

From the XRD measurement of the tempered Fe-0.3N specimen, only the diffraction peaks derived from bcc structure, implying martensite phase was observed in the as-quenched specimen, and the diffraction peaks derived from precipitates were not confirmed. The diffraction peaks derived from bcc and that from  $\alpha''$ -Fe<sub>16</sub>N<sub>2</sub> phase were obtained in the specimen tempered at 100 °C and 200 °C, respectively, whereas that derived from bcc and  $\gamma'$ -Fe<sub>4</sub>N were confirmed in the specimen tempered at more than 300 °C.

Fig. 2 (a) shows the volume fraction change of iron nitrides for the Fe-0.3N specimen during

tempering and calculated volume fraction by Thermo-Calc software using TCFE7 database and (b) is volume fraction of iron nitrides for the specimens with alloy addition. In the Fe-0.3N specimen, the volume fraction of  $\alpha''$ -Fe<sub>16</sub>N<sub>2</sub> increased with increasing tempering temperature, and reached the maximum value of 5 % at 200 °C, then decreased. The volume fraction of  $\gamma'$ -Fe<sub>4</sub>N gradually increased with increasing tempering temperature and reached 5 % at 300 °C, then it became constant in further increment of tempering temperature. The calculated  $\gamma'$ -Fe<sub>4</sub>N volume fraction of the Fe-0.3N specimen at 500 °C by Thermo-calc is 4.9 %, showing a good agreement with the measurement. In the Si and Mo-added specimens, the volume fraction of  $\gamma'$  showed a similar trend to the result of Fe-0.3 N specimen. The volume fraction of  $\gamma'$ -Fe<sub>4</sub>N in these specimens increased with increasing tempering temperature and reached the maximum at 300 °C and 500 °C, respectively. In the Mn-added specimen, the volume fraction of  $\gamma'$ -Fe<sub>4</sub>N increased with increasing tempering temperature and showed a higher value than Fe-0.3N specimen at temperatures higher than 400 °C and reaches to 5.5 % at 500 °C. In the Cr-added specimen, the volume fraction gradually increased with increasing tempering temperature up to 300 °C, and reached the maximum (about 4 %) at 300 °C, and then decreased in further increment of the tempering temperature. The volume fractions of  $\gamma'$  of the Si, Cr and Mo-added specimen were lower than the Fe-0.3N specimen in spite that there was no large difference in the calculated solubility limit of nitrogen in the ferrite phase at 500 °C among those alloys. On the other hand, although the maximum value of volume fraction of  $\alpha''$  was different for all samples, it showed the similar tendency and the maximum volume fraction was obtained by tempering at 200 °C, and the volume fraction decreased with subsequent increasing tempering temperature.

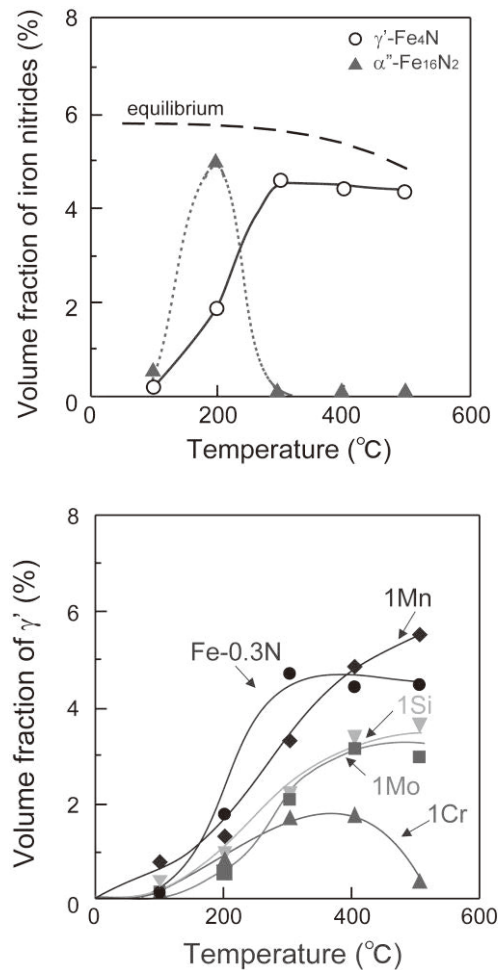


Fig. 2 (a) Measured and calculated volume fractions of  $\gamma'$ -Fe<sub>4</sub>N and  $\alpha''$ -Fe<sub>16</sub>N<sub>2</sub> in the Fe-0.3N specimen and (b)  $\gamma'$  fraction in the alloyed element specimens at various tempering temperatures.

Fig. 3 shows (a) the hardness change of the Fe-0.3N obtained in the present study. The result was compared with the hardness of the Fe-C binary alloy reported by Grange et al [8]. In the Fe-0.3N specimen, the hardness of as-quenched specimen was around 500 HV and it monotonously decreased with increasing the tempering temperature and showed 300 HV at 400 °C. Then, the hardness became constant in further increment of the tempering temperature. In comparison with Fe-C alloys, the hardness of as-quenched Fe-0.3N specimen shows almost same value to the Fe-0.2C specimen as shown

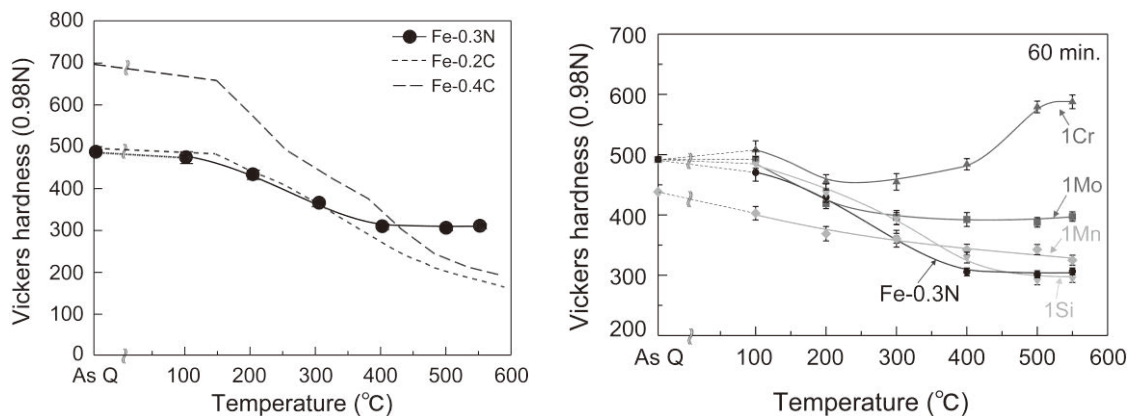


Fig. 3 (a) Comparison of hardness change of Fe-N and Fe-C specimens and (b) alloying element added specimens.

in Fig. 3(a). This result exhibited similar trend to the previous report [9]. The hardness of Fe-C alloys also decreased by tempering, and similar hardness changes to the Fe-0.3N specimen was obtained up to the tempering temperature of 300 °C. However, the hardness of Fe-0.3N specimen became higher than both of the Fe-0.2C and Fe-0.4C specimen in the tempering temperature around 400 °C, showing a good resistance to tempering softening. Fig. 3(b) shows the hardness change of alloyed specimen by tempering. In the Si-added specimen, although it was slightly harder in the temperature range between 100 °C and 500 °C, it showed similar hardness change to the Fe-0.3N specimen. The Mo-added specimen showed a similar trend to the Fe-0.3N specimen until 200 °C. However, the obtained hardness did not change in further increment of tempering temperature. In the Mn-added specimen, the hardness of as-quenched specimen was lower than the other specimens. Although the hardness monotonously decreased with increasing tempering temperature, its decreasing rate was low. On the other hand, in the case of the Cr-added specimen, the hardness increased in tempering temperature more than 200 °C and clearly showed the secondary hardening. It is thought that this secondary hardening is caused by the precipitation of CrN. The maximum hardness value of 590 HV was obtained at 500 °C.

The dislocation density of each specimen was calculated by the modified Warren-Averbach method [10, 11] from the XRD measurement result. It was found that the dislocation density was around  $4.5 \times 10^{15} \text{ m}^{-2}$  in the alloys as-quenched and also tempered a temperature between 100 °C and 200 °C, and the difference among the alloys was very small as shown in Fig. 4. On the other hand, the dislocation density remarkably decreased at 300 °C, and it monotonously decreased in further increment of tempering temperature in most of the alloys used. However, the Cr-added specimen showed a higher dislocation density than the other samples after tempering at 500 °C, this is considered to be the influence of the peak broadening due to the coherency strain and retardation of dislocation recovery accompanying the precipitation of CrN.

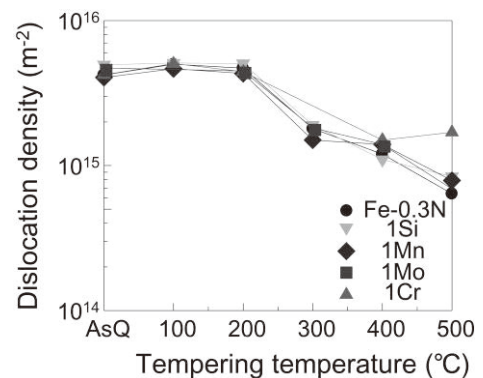


Fig. 4 Change in dislocation density by tempering.

#### 4. CONCLUSIONS

The tempering behavior of Fe-N alloy and the effect of alloying element were investigated. In the Fe-0.3N alloy, the hardness monotonously decreased with increasing tempering temperature due to the decrease of nitrogen concentration caused by the precipitation of  $\alpha$ '-Fe<sub>16</sub>N<sub>2</sub> and  $\gamma$ '-Fe<sub>4</sub>N. In comparison with the Fe-C alloy, the nitrogen martensite showed resistance to temper softening at above 400 °C. In addition, the transition of  $\alpha$ '-Fe<sub>16</sub>N<sub>2</sub> to  $\gamma$ '-Fe<sub>4</sub>N occurred at 200 °C. By the addition of alloying elements, the resistance to temper softening occurred in the order of Cr > Mo > Mn >> Si, and Cr-added specimen clearly showed secondary hardening due to the precipitation of CrN. The dislocation density of all alloys was decreased by the tempering at temperatures higher than 300 °C, and the reduction rate of the Cr-added specimen was smaller than other alloys.

#### REFERENCES

- [1] T. Bell and S. W. Owen: J. Iron Steel Inst., 205 (1967), 428.
- [2] K. Takano, M. Sakakibara, T. Matsui and S. Takaki: Tetsu-to-Hagané, 86 (2000), 123.
- [3] L. Cheng; E. J. Mittemeijer, Metall. Trans A, 21A 13-26 (1990)
- [4] M. B. Horovitz, F. Beneduceneto, A. Garbogini and A. P. Tschiptschin, ISIJ Int. 36 840-845 (1996)
- [5] N. H. K. Luan, H. Nakashima, T. Tsuchiyama and S. Takaki : Tetsu-to-Hagané, 98 (2012), 25.
- [6] V.G.Gavriljuk and H.Berns : High Nitrogen Steels, Springer, Verlag Belrin Heidelberg, (1999).
- [7] J. Takeuchi, T. Iguchi and T. Ishihara: Netsu Shori 21 (1981) 26
- [8] R.A.Grange, C.R.Hribal and L.F.Porter : Metall. Trans. A, 8A (1977), 1775.
- [9] M. Chiba, G. Miyamoto and T. Furuahara: J. Japan Inst. Metals, 76 (2012), 256.
- [10] B. E. Warren and B. L. Averbach: J. Appl. Phys., 21 (1950), 595.
- [11] B. E. Warren and B. L. Averbach: J. Appl. Phys., 23 (1952), 497.